NANO LETTERS

Letter

pubs.acs.org/NanoLett

Enhanced Magnetoresistance in Molecular Junctions by Geometrical Optimization of Spin-Selective Orbital Hybridization

David Rakhmilevitch,[†] Soumyajit Sarkar,[‡] Ora Bitton,[§] Leeor Kronik,[‡] and Oren Tal*[,†]

[†]Department of Chemical Physics, [‡]Department of Materials and Interfaces, and [§]Department of Chemical Research Support, Weizmann Institute of Science, Rehovot, Israel

Supporting Information

ABSTRACT: Molecular junctions based on ferromagnetic electrodes allow the study of electronic spin transport near the limit of spintronics miniaturization. However, these junctions reveal moderate magnetoresistance that is sensitive to the orbital structure at their ferromagnet−molecule interfaces. The key structural parameters that should be controlled in order to gain high magnetoresistance have not been established, despite their importance for efficient manipulation of spin transport at the nanoscale. Here, we show that single-molecule junctions based on nickel electrodes and benzene molecules can yield a significant anisotropic magnetoresistance of up to ∼200% near the conductance quantum G_0. The measured magnetoresistance is mechanically tuned by changing the distance between the electrodes, revealing a nonmonotonic response to junction elongation. These findings are ascribed with the aid of first-principles calculations to variations in the metal−molecule orientation that can be adjusted to obtain highly spin-selective orbital hybridization. Our results demonstrate the important role of geometrical considerations in determining the spin transport properties of metal−molecule interfaces.

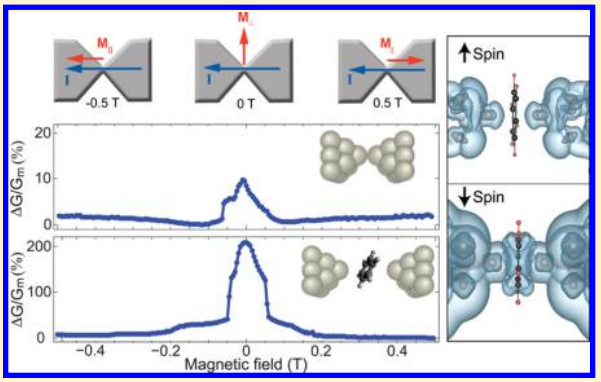

KEYWORDS: *Spintronics, spinterface, molecular electronics, magnetoresistance, molecular junction, spin transport*

Spintronics has a large impact on daily life, being the backbone of computer hard drives.[1] The reduction in size of spintronic elements is of central importance for efficient information processing, as well as for demonstrating intriguing physical phenomena.[2−6] In this respect, magnetoresistance measurements across molecular junctions provide a useful testbed for spin transport at the nanoscale.[7] Previous studies showed that magnetoresistance in molecular junctions is sensitive to the orbital structure at the metal−molecule interfaces.[8−10] However, the structural aspects that should be considered in order to gain optimal magnetoresistance enhancement have not been studied. This information is necessary in order to develop a practical methodology for controlled spin transport across metal−molecule interfaces in a variety of nanoscale molecular junctions and organic spintronic devices. Here, we show that anisotropic magnetoresistance (AMR) in molecular junctions can be enhanced by more than an order of magnitude with respect to the corresponding bare atomic junctions, while mechanical modifications of the junction efficiently tune the obtained magnetoresistance. With the aid of first-principle calculations, these effects are explained by spin-selective orbital hybridization that can be optimized by tuning the relative orientation between the metal electrodes and the molecule. Our findings shed light on the structural and geometrical conditions at metal−molecule interfaces that are required for optimal magnetoresistance.

The mechanism underlying AMR in the bulk is anisotropic scattering of electrons as a result of spin−orbit interaction, which depends on the relative orientation of the magnetization and the electronic current. Generally, stronger scattering is expected for current aligned with the conductor magnetization, leading to higher resistivity in comparison to current perpendicular to the magnetization (Figure 1, bottom left inset). The change in resistance for bulk ferromagnetic metals is small and does not exceed 5%.[11] Interestingly, when the size of a ferromagnet is reduced to the atomic-scale, the AMR response is enhanced to 10−15%.[12,13] This enhancement was ascribed to the high sensitivity of the local electronic structure at the atomic constriction to the magnetization direction, resulting in large variations in the electronic transmission.[14−16] While larger than the bulk response, AMR in atomic-scale devices based on metallic ferromagnetic electrodes is limited by their moderate injection of spin current. The conductance of these metals is dominated by the insignificantly spin-polarized sp bands rather than by the spin-polarized d bands, resulting in moderate conductance variations in response to magnetic manipulations.[11] The limited spin injection from ferromagnetic metals is a general drawback, leading to the incorporation of

Received: November 16, 2015
Revised: February 4, 2016

DOI: 10.1021/acs.nanolett.5b04674
Nano Lett. XXXX, XXX, XXX−XXX

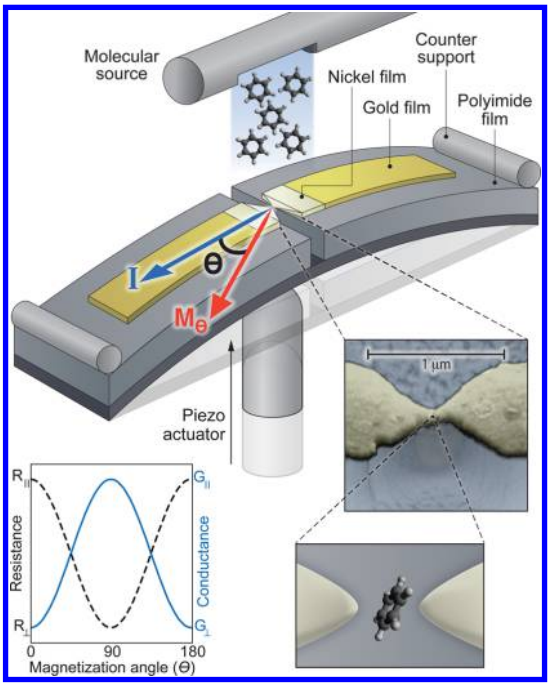

Figure 1. Schematic description of the measurement setup. The sample is composed of lithographically-defined gold electrodes, connected by a microscale ferromagnetic Ni constriction. The central panel depicts a scanning electron microscope image of the constriction and the suspended bridge. A three-point bending mechanism is used to controllably break the constriction so as to form atomic and tunnel junctions. Benzene molecules are introduced to the junctions via a molecular source in order to form molecular junctions (schematically depicted in the bottom right panel). By applying an external magnetic field the relative angle (θ) between the magnetization of the junction and the current across it is changed, affecting the conductance (or resistance) as schematically illustrated in the bottom left inset for a bulk contact.

sophisticated structures and exotic materials[17,18] in order to increase the magnetoresistance and therefore the sensitivity of spintronic devices. This limitation can be confronted by taking advantage of the chemical binding between π-conjugated molecules and ferromagnetic metals to promote transport via the frontier spin-polarized d-orbitals of ferromagnetic electrodes.[9,19,20] Yet, having such a spin-selective orbital hybridization is only a prerequisite and geometrical aspects should be taken into consideration.

We use a break-junction setup at cryogenic temperatures (5.9 K) to study AMR in nanoscale contacts, as well as in atomic and molecular junctions using the same sample. This approach allows for a reliable comparison between the AMR properties of the three systems. The samples are made of two gold leads connected by a microscale ferromagnetic nickel (Ni) section (Figure 1). The metallic structure is firmly attached to a bendable substrate, excluding a nanoscale segment at the center of the Ni constriction. With the aid of a three-point bending mechanism, the suspended Ni segment is stretched and broken in cryogenic vacuum, exposing two ultraclean Ni apexes. The distance between these electrodes can be adjusted with sub-angstrom resolution to repeatedly form single-atom junctions with different atomic tip configurations. Molecular junctions are obtained by introducing benzene molecules in situ via a molecular source. Our sample design is optimized to efficiently suppress undesired magnetostrictive effects that can contribute to the measured magnetoresistance by changing the distance between the electrodes. This is achieved by minimizing the ferromagnetic section of the junction and in particular the freely suspended region.[21] The negligible role of magnetostriction is verified by the absence of systematic changes in magnetoresistance in control experiments performed on the bare Ni junctions at the onset of tunneling conductance. Further details can be found in the Supporting Information.

AMR can be measured by changing the direction of sample magnetization with respect to the current with the aid of a rotating magnetic field. Relevant results based on this measurement technique are presented in the Supporting Information for atomic and molecular junctions. However, when measuring atomic-scale junctions, this approach promotes abrupt conductance variations that may stem (among other possibilities) from local atomic and molecular rearrangements induced by the rotating magnetic field,[22] rather than from intrinsic AMR. To avoid ambiguity, we adopted a simpler yet well-established measurement scheme.[23,24] We first analyzed the conductance response to magnetic field sweeps along the three principal axes of our junctions and identified that near zero magnetic field the junctions are spontaneously magnetized perpendicular to the junction axis and in its plane[25] (as discussed thoroughly in the Supporting Information). Then, the conductance was measured while the magnetic field is swept along the sample axis (Figure 2a). The magnetization of

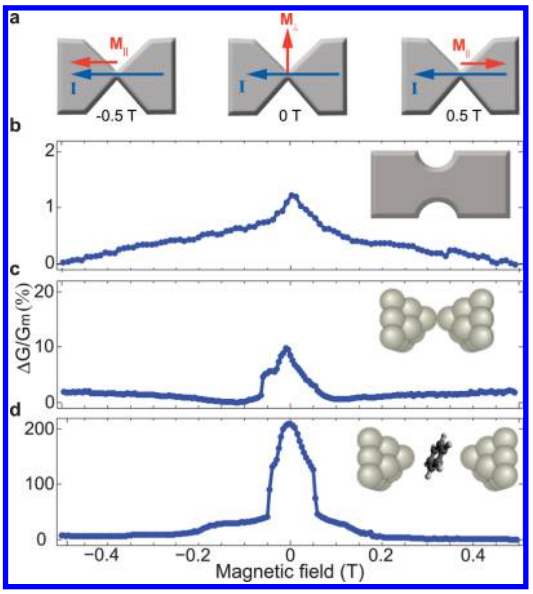

Figure 2. (a) Schematic description of the junction magnetization during a sweep of magnetic field along the sample axis. AMR measured on (b) a nanoscale contact ($G_m = 98G_0$), (c) a Ni atomic junction ($G_m = 1.36G_0$), and (d) a Ni/benzene molecular junction ($G_m = 0.42G_0$). The similar trend of the relative conductance for the atomic and molecular junctions suggests that the easy axis for magnetization is the same in both cases.

the sample is initially aligned antiparallel to the current by applying a magnetic field of 0.5 T in this direction, leading to a low conductance. As the magnetic field is reduced to zero the magnetization is spontaneously aligned perpendicular to the current, resulting in a higher conductance. Finally, when the magnetic field is increased in the opposite direction the magnetization is aligned in parallel to the current. This scheme yields fairly smooth conductance variations as a function of

DOI: 10.1021/acs.nanolett.5b04674
Nano Lett. XXXX, XXX, XXX−XXX

magnetic field, for both atomic and molecular junctions, indicating the lack of abrupt atomic and molecular rearrangements in the junction constriction.

In atomic-scale transport measurements, it is customary to focus on conductance rather than resistance. Therefore, the AMR response is defined as $\Delta G/G_m = (G_{\parallel} - G_{\perp})/G_{\parallel} = (R_{\perp} - R_{\parallel})/R_{\perp}$ where G_i and R_i ($i = \parallel, \perp$) are the conductance and resistance parallel or perpendicular to the current direction and $G_m = G_{\parallel}$ is the minimal conductance. As a first step, we focus on the AMR response of a Ni nanoscale contact. In this regime, near zero magnetic field there are multiple magnetic domains in the vicinity of the contact and the magnetic field acts to align them with the junction axis. Figure 2b presents the AMR ratio as a function of magnetic field for a nanoscale contact with a zero-bias differential conductance of 98.0 G_0 ($G_0 \cong 1/12.9\text{K}\ \Omega$ is the conductance quantum). An AMR ratio of 1.23% is obtained, which is in agreement with the typical AMR found for bulk Ni.[11] In order to analyze the AMR response of atomic junctions, the junction was partially broken in a controllable fashion while measuring the conductance. During this process the number of atoms in the cross-section of the Ni constriction was gradually reduced up to a single-atom contact that is characterized by a typical conductance of 1.2−1.4 G_0.[26,27] Figure 2c shows that the AMR response is increased to 9.8% when an atomic junction is formed. Similar AMR enhancement was reported previously for atomic-scale junctions[12,13] and was attributed to the enhanced sensitivity of conductance across an atomic-scale constriction to magnetization-induced variations in the local density of states, or to a possible enhancement of spin−orbit interaction due to the low atomic-coordination.[14−16] Further elongation of the junction resulted in breaking of the contact and formation of a tunnel junction (see Supporting Information).

In order to study the AMR response of a molecular junction the examined atomic junction was further elongated until it was broken. At this point, benzene molecules were introduced into the junction by sublimation from a molecular source and the interelectrode separation was adjusted to form a molecular junction. The presence of a molecule in the junction was initially verified for each junction realization by measuring a stable conductance value smaller than the typical conductance of bare Ni atomic junctions. Further verification was obtained by detecting the molecular signature of vibration activation in the conductance of the junction (see Supporting Information). Figure 2d presents an AMR measurement taken after the formation of a molecular junction. The AMR response of the molecular junction reaches 208%, more than 1 order of magnitude higher than the AMR obtained for the corresponding atomic Ni junction (see Supporting Information for statistical data). This maximal AMR response is higher than previously reported magnetoresistance ratios found for single molecule junctions.[9,10,28−30]

The structure of molecular junctions evolves when the interelectrode distance is increased.[31] To characterize the effect of structural modifications on magneto-transport, we studied the response of the AMR ratio to junction elongation. The interelectrode separation was increased in sub-angstrom sequential steps of 0.1 Å, while the conductance and AMR response were measured at each step. As can be seen in Figure 3a, the conductance is monotonically reduced when the junction is elongated. In contrast, the AMR is first enhanced, reaching an optimal value at $G_m \sim 0.4G_0$ (Figure 3b), and decreases afterward. This behavior indicates that the AMR ratio

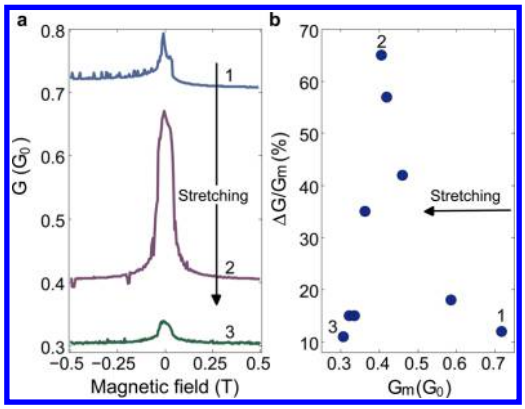

Figure 3. (a) Selected magnetoconductance curves for different junction elongations. (b) AMR ratio for the entire stretching sequence, partially shown in (a), as a function of G_m; the decrease in G_m is due to a monotonic increase in electrode separation (further details appear in the Supporting Information).

is optimal in a certain molecular junction configuration, allowing mechanical tunability of the AMR effect. We note that the nonmonotonic AMR response is consistent with the negligible role of magnetostriction in our design. This undesired effect is expected to yield monotonically increasing magnetoresistance as the conductance is reduced by stretching toward the tunneling regime.

To shed light on the origin of the high AMR in our single molecule junctions, as well as its evolution during junction elongation we performed density functional theory (DFT) based first-principles calculations (see Supporting Information). We note that related transport calculations were recently reported for a model system of a Ni-benzene junction.[32] Figure 4a shows the spin-resolved projected density of states on the π (PDOS$^{\pi}$) and σ (PDOS$^{\sigma}$) benzene orbitals, at an interelectrode distance of 7.2 Å for which the junction has a minimum total energy (see Supporting Information). At the Fermi energy, the energy relevant for transport, PDOS$^{\pi}$ is considerably larger than PDOS$^{\sigma}$. Moreover, in contrast to PDOS$^{\sigma}$, the different PDOS$^{\pi}$ for the spin up and down channels indicate a clear spin-polarization near the Fermi energy. Because the isolated molecule has no magnetic moment and charge transfer between the molecule and the electrodes is negligible (see Supporting Information), the observed spin-polarization should stem from hybridization with the magnetic electrodes.[20,33,34]

A better understanding of this effect can be gained by looking at the corresponding real-space plot of the spin-resolved charge density around the Fermi energy (Figure 4b). For the spin down channel, an efficient hybridization between the frontier d-orbitals of the Ni electrodes and the π-orbitals of the molecule is clearly visible. This is in clear contrast to the spin up channel, showing minor orbital hybridization between the molecule and the electrodes. The significantly different hybridization for the spin up and spin down channels leads to high spin polarization (further details appear in the Supporting Information). Similar selective π−d hybridization was revealed experimentally for benzene molecules adsorbed on Ni surfaces.[35] Because of anisotropic spin−orbit coupling in ferromagnetic atomic-scale junctions, spin-polarized states are shifted with respect to the Fermi energy in response to changes in the magnetization direction.[14−16,32] As a result, the dominant role of the spin-polarized π−d hybridized states at the Fermi energy is expected to enhance the AMR response of the molecular junction.

DOI: 10.1021/acs.nanolett.5b04674
Nano Lett. XXXX, XXX, XXX−XXX

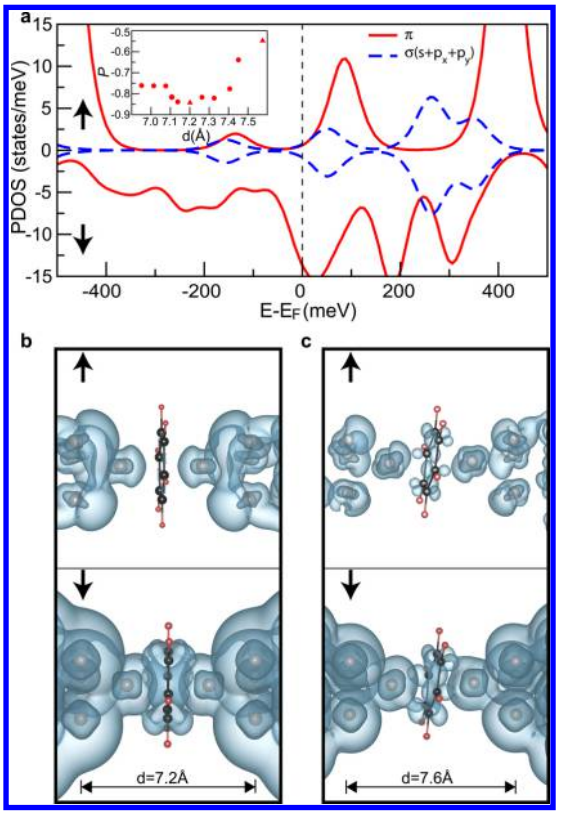

Figure 4. (a) Calculated density of states projected on the π- (solid, red) and σ- (dashed, blue) orbitals of the benzene molecule for an interelectrode separation of 7.2 Å. Inset: calculated P for different interelectrode separation, d. The values of P for interelectrode distances of 7.2 and 7.6 Å, discussed in the text, are marked with triangles. (b,c) Spin-resolved charge density plots for an energy window of 100 meV around the Fermi energy for two junction configurations with an interelectrode distance of 7.2 Å (b) and 7.6 Å (c), respectively.

The observed tunable AMR can be explained by the directionality of d-orbitals in space, dictating that the π−d hybridization is sensitive to variations in the mutual orientation of these orbitals.[31,36] The degree of spin polarization of PDOS$^{\pi}$ at the Fermi energy can indicate the relevant spin selectivity for transport. This quantity is defined as $P = \frac{\mathrm{PDOS}^{\pi}_{\uparrow}(E_F) - \mathrm{PDOS}^{\pi}_{\downarrow}(E_F)}{\mathrm{PDOS}^{\pi}_{\uparrow}(E_F) + \mathrm{PDOS}^{\pi}_{\downarrow}(E_F)}$ and it is presented in the inset of Figure 4a as a function of electrode separation. Similar to the measured AMR, the spin polarization P is clearly subjected to nonmonotonic variations as a function of junction elongation. Comparison between the spin-resolved charge density plots for compact (Figure 4b) and extended (Figure 4c) junction configurations reveals that the molecule tilts with respect to the electrode axis as a result of junction elongation. In the extended configuration, the overall hybridization between the molecule and the electrode frontier orbitals is reduced, and non-negligible π−d hybridization is now found for both spin up and spin down electrons, resulting in the observed decrease in spin polarization. For relatively compact junction configurations with measured conductance above $0.4G_0$ (Figure 3b), the reduction in P indicates a less dominant contribution of spin-polarized states to the conductance and hence moderate AMR. Beyond this effect, for close enough electrodes some reduction of AMR may result from poorly spin-polarized tunneling conductance between the Ni apexes. This background conductance, which is dominated by the Ni frontier s-orbitals, is rather insensitive to magnetization variations.[32] The exemplified structural flexibility of the molecular junction can therefore be used to modify the orbital hybridization in the junction and optimize the AMR response.

To conclude, significantly high and tunable AMR was demonstrated in Ni/benzene molecular junctions. Our analysis indicate an optimal molecular orientation with respect to the ferromagnetic metal electrodes, in which a maximal AMR is achieved due to efficient spin-selective orbital hybridization. These findings demonstrate the importance of geometrical considerations in determining the spin transport properties at metal−molecule interfaces and open the door for controlled magnetoresistance by geometrical modifications at such interfaces.

■ ASSOCIATED CONTENT

Supporting Information

The Supporting Information is available free of charge on the ACS Publications website at DOI: 10.1021/acs.nanolett.5b04674.

Device fabrication and molecule insertion schemes; the role of magneto-elastic effects in our junctions; AMR measurements in a rotating magnetic field; determination of the easy-axis in our junctions; establishing transport through the molecule using inelastic electron spectroscopy; the effects of variable molecular configurations; description of computational methodology and details of the model system; analysis of charge transfer between the molecule and the electrodes; and additional real-space spin-resolved charge density plots. (PDF)

■ AUTHOR INFORMATION

Corresponding Author

*E-mail: oren.tal@weizmann.ac.il.

Author Contributions

D.R. and O.T. conceived the project and designed the experiments. D.R. constructed the measurement setups, performed the experiments, and analyzed the extracted data. O.B helped in designing the experiment and, together with D.R., fabricated the samples. S.S. and L.K. performed the calculations and participated together with D.R. and O.T. in the overall analysis of the results. D.R. and O.T. wrote the paper and all coauthors commented on the manuscript.

Notes

The authors declare no competing financial interest.

■ ACKNOWLEDGMENTS

D.R. and O.T. are grateful to E. Scheer, F. Striegl, and T. Pietch for their valuable help with the lithography process. O.T. and L. K. thank the Harold Perlman Family for their support and acknowledge funding by the Israel Science Foundation (Grant 089/15). O.T. and L.K. further acknowledge support from the Minerva Foundation (Grant 711136) and the Lise Meitner Minerva Center for Computational Chemistry, respectively.

■ REFERENCES

(1) Wolf, S. A.; Awschalom, D. D.; Buhrman, R. A.; Daughton, J. M.; Von Molnar, S.; Roukes, M. L.; Chtchelkanova, A. Y.; Treger, D. M. *Science* **2001**, *294*, 1488−1495.

(2) Sahoo, S.; Kontos, T.; Furer, J.; Hoffmann, C.; Gräber, M.; Cottet, A.; Schönenberger, C. *Nat. Phys.* **2005**, *1*, 99−102.

DOI: 10.1021/acs.nanolett.5b04674
Nano Lett. XXXX, XXX, XXX−XXX

(3) Loth, S.; Baumann, S.; Lutz, C. P.; Eigler, D. M.; Heinrich, A. J. *Science* **2012**, *335*, 196−199.
(4) Sankey, J. C.; Cui, Y. T.; Sun, J. Z.; Slonczewski, J. C.; Buhrman, R. A.; Ralph, D. C. *Nat. Phys.* **2008**, *4*, 67−71.
(5) Rocha, A. R.; Garcia-Suarez, V. M.; Bailey, S. W.; Lambert, C. J.; Ferrer, J.; Sanvito, S. *Nat. Mater.* **2005**, *4*, 335−339.
(6) Ziegler, M.; Néel, N.; Lazo, C.; Ferriani, P.; Heinze, S.; Kröger, J.; Berndt, R. *New J. Phys.* **2011**, *13*, 085011.
(7) Aradhya, S. V.; Venkataraman, L. *Nat. Nanotechnol.* **2013**, *8*, 399−410.
(8) Raman, K. V.; Kamerbeek, A. M.; Mukherjee, A.; Atodiresei, N.; Sen, T. K.; Lazić, P.; Caciuc, V.; Michel, R.; Stalke, D.; Mandal, S. K.; Blügel, S.; Münzenberg, M.; Moodera, J. S. *Nature* **2013**, *493*, 509−513.
(9) Schmaus, S.; Bagrets, A.; Nahas, Y.; Yamada, T. K.; Bork, A.; Bowen, M.; Beaurepaire, E.; Evers, F.; Wulfhekel, W. *Nat. Nanotechnol.* **2011**, *6*, 185−189.
(10) Li, J. J.; Bai, M. L.; Chen, Z. B.; Zhou, X. S.; Shi, Z.; Zhang, M.; Ding, S.-Y; Hou, S.-M; Schwarzacher, W.; Nichols, R. J.; Mao, B. W. *J. Am. Chem. Soc.* **2015**, *137*, 5923−5929.
(11) McGuire, T.; Potter, R. *IEEE Trans. Magn.* **1975**, *11*, 1018−1038.
(12) Bolotin, K. I.; Kuemmeth, F.; Ralph, D. C. *Phys. Rev. Lett.* **2006**, *97*, 127202.
(13) Keane, Z. K.; Yu, L. H.; Natelson, D. *Appl. Phys. Lett.* **2006**, *88*, 062514.
(14) Velev, J.; Sabirianov, R. F.; Jaswal, S. S.; Tsymbal, E. Y. *Phys. Rev. Lett.* **2005**, *94*, 127203.
(15) Jacob, D.; Fernández-Rossier, J.; Palacios, J. J. *Phys. Rev. B: Condens. Matter Mater. Phys.* **2008**, *77*, 165412.
(16) Häfner, M.; Viljas, J. K.; Cuevas, J. C. *Phys. Rev. B: Condens. Matter Mater. Phys.* **2009**, *79*, 140410.
(17) Barraud, C.; Seneor, P.; Mattana, R.; Fusil, S.; Bouzehouane, K.; Deranlot, C.; Graziosi, P.; Heuso, L.; Bergenti, I.; Dediu, V.; Petroff, F.; Fert, A. *Nat. Phys.* **2010**, *6*, 615−620.
(18) Sanvito, S. *Nat. Phys.* **2010**, *6*, 562−564.
(19) Smogunov, A.; Dappe, Y. J. *Nano Lett.* **2015**, *15*, 3552−3556.
(20) Atodiresei, N.; Brede, J.; Lazić, P.; Caciuc, V.; Hoffmann, G.; Wiesendanger, R.; Blügel, S. *Phys. Rev. Lett.* **2010**, *105*, 066601.
(21) Gabureac, M.; Viret, M.; Ott, F.; Fermon, C. *Phys. Rev. B: Condens. Matter Mater. Phys.* **2004**, *69*, 100401.
(22) Shi, S.-F.; Ralph, D. C. *Nat. Nanotechnol.* **2007**, *2*, 522−523.
(23) Gil, W.; Görlitz, D.; Horisberger, M.; Kötzler, J. *Phys. Rev. B: Condens. Matter Mater. Phys.* **2005**, *72*, 134401.
(24) Leighton, C.; Song, M.; Nogués, J.; Cyrille, M. C.; Schuller, I. K. *J. Appl. Phys.* **2000**, *88*, 344−347.
(25) Egle, S.; Bacca, C.; Pernau, H. F.; Huefner, M.; Hinzke, D.; Nowak, U.; Scheer, E. *Phys. Rev. B: Condens. Matter Mater. Phys.* **2010**, *81*, 134402.
(26) Pauly, F.; Dreher, M.; Viljas, J. K.; Häfner, M.; Cuevas, J. C.; Nielaba, P. *Phys. Rev. B: Condens. Matter Mater. Phys.* **2006**, *74*, 235106.
(27) Untiedt, C.; Dekker, D.M. T.; Djukic, D.; van Ruitenbeek, J. M. *Phys. Rev. B: Condens. Matter Mater. Phys.* **2004**, *69*, 081401.
(28) Yamada, R.; Noguchi, M.; Tada, H. *Appl. Phys. Lett.* **2011**, *98*, 053110.
(29) Kawahara, S. L.; Lagoute, J.; Repain, V.; Chacon, C.; Girard, Y.; Rousset, S.; Smogunov, A.; Barreteau, C. *Nano Lett.* **2012**, *12* (9), 4558−4563.
(30) Yoshida, K.; Hamada, I.; Sakata, S.; Umeno, A.; Tsukada, M.; Hirakawa, K. *Nano Lett.* **2013**, *13* (2), 481−485.
(31) Kiguchi, M.; Tal, O.; Wohlthat, S.; Pauly, F.; Krieger, M.; Djukic, D.; Cuevas, J. C.; van Ruitenbeek, J. M. *Phys. Rev. Lett.* **2008**, *101*, 046801.
(32) Otte, F.; Heinze, S.; Mokrousov, Y. *Phys. Rev. B: Condens. Matter Mater. Phys.* **2015**, *92*, 220411.
(33) Wende, H.; Bernien, M.; Luo, J.; Sorg, C.; Ponpandian, N.; Kurde, J.; Miguel, J.; Piantek, M.; Xu, X.; Eckhold, Ph.; Kuch, W.; Baberschke, K.; Panchmatia, P. M.; Sanyal, B.; Oppeneer, P. M.; Eriksson, O. *Nat. Mater.* **2007**, *6*, 516−520.
(34) Brede, J.; Atodiresei, N.; Kuck, S.; Lazić, P.; Caciuc, V.; Morikawa, Y.; Hoffmann, G.; Blügel, S.; Wiesendanger, R. *Phys. Rev. Lett.* **2010**, *105*, 047204.
(35) Demuth, J. E.; Eastman, D. E. *Phys. Rev. B* **1976**, *13*, 1523−1527.
(36) Yelin, T.; Vardimon, R.; Kuritz, N.; Korytár, R.; Bagrets, A.; Evers, F.; Kronik, L.; Tal, O. *Nano Lett.* **2013**, *13*, 1956−1961.

DOI: 10.1021/acs.nanolett.5b04674
Nano Lett. XXXX, XXX, XXX−XXX